Global NEST Journal, Vol 27, No X, pp 1-13

Characterization of high-temperature carbonization products of sludge mixed with corn cobs

Yuhao Lu[1], He Li[1]*,Zhiren Wu[2] and Xiaoyun Ma[1]
[1]School of Civil Engineering, Southeast University, Nanjing 211189, China
[2]School of Environmental and Safety Engineering, Jiangsu University, Zhenjiang 212013, China
Received: 03/04/2025, Accepted: 17/04/2025, Available online: 29/04/2025
*to whom all correspondence should be addressed: e-mail: ericlihe@seu.edu.cn
https://doi.org/10.30955/gnj.07520

Graphical abstract

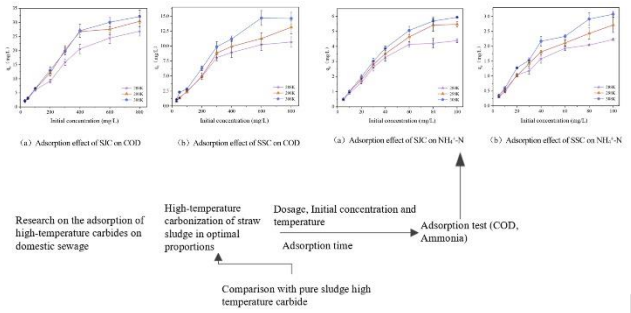

Abstract

There exists a mutually reinforcing relationship between sludge and corn cob, and their combined treatment products have high potential for application. This paper focuses on the comprehensive characterization of the properties of the combined high-temperature carbonization products of sludge and corn cob and explores the effectiveness of high-temperature carbonization on the main pollutant indexes in the water treatment process. The optimal ratio (W_{sludge}: $W_{corn\ cob}$ = 4:1) of dried corn cob sludge high-temperature carbonization (SJC) prepared at pyrolysis temperature (800℃), heating rate (5℃/min) and holding time (120 min) was used as the experimental group, and pure sludge high-temperature carbonization (SSC) was used as the control group, and the adsorption effect and adsorption mechanism of SJC and SSC on COD and NH_4^+-N in the concentration range of simulated domestic wastewater were investigated. The adsorption effects of SJC and SSC on COD and NH_4^+-N in the concentration range of simulated domestic wastewater were investigated. The results showed that the adsorption amount of COD and NH_4^+-N by SJC was larger than that of SSC, and the removal rate of SJC for COD solution with an initial concentration of 300 mg/L could be more than 50% at 298 K, and that of NH_4^+-N solution with a concentration of 40 mg/L could be up to 70%.

Keywords: High Temperature Carbonization; Sludge; Corn Cob; Adsorption; Resource Utilization

1. Introduction

With the rapid development of industry and agriculture in China, the production of sludge and corn cobs has been growing rapidly. In order to strengthen the construction of ecological civilization and promote the comprehensive green transformation (Zongshu 2024) and development of the society and economy (Selvanarayanan *et al.* 2024), the state has issued a series of policies and norms in recent years in order to promote the rational disposal and comprehensive utilization of sludge and corn cobs. Studies have shown that there is a mutually reinforcing relationship between sludge and corn cobs, and their joint treatment products have a high potential for application, but at present, there are limitations in the traditional treatment and disposal options for sludge, and there are fewer studies on resourcing. Therefore, this paper focuses on the comprehensive characterization of the properties of the combined high temperature carbonation products of sludge and corn cobs and explores the effectiveness of high temperature carbonation on the main pollution indicators during water treatment(Venkatraman *et al.* 2024). This study is very important to understand the direction of high-temperature carbonization and subsequent resource utilization, and to implement the treatment route of 'waste for waste'.

There is a mutually reinforcing relationship between sludge and corn cob. Corn cobs have a high carbon-to-nitrogen ratio and contain a lot of hemicellulose and cellulose, which far exceeds the carbon content in dry sludge. Corn cob materials are similar to skeleton particles such as lignite and fly ash, with good porosity and hard structure, so corn cob materials have the potential to be used as skeleton particles to condition sludge dewatering (Cai *et al.* 2018). Due to the high carbon content of corn cobs, researchers globally are exploring the utilization of corn cobs in the production of adsorbent materials, so that they can play a role in the related fields of water treatment(Suresh *et al.* 2025). The high carbon content of agricultural corn cob itself will make up for the shortcomings of low carbon content of municipal sludge (Yang *et al.* 2024), and the colloidal characteristics of the

sludge itself will also improve the shortcomings of corn cob (Iheanacho *et al.* 2023) that are not easy to form, and the complementary effect between the two makes the adsorbent have better performance.

Sludge carbonization (Merzari *et al.* 2019) is also known as "thermal decomposition" or "cracking". It is a process in which the water of the cells in the biochemical sludge is forcibly removed by pyrolysis under a certain temperature and pressure, and the organic matter is converted into non-condensable gas (Wang *et al.* 2020) , water vapor and carbon, so that the proportion of carbon content in the sludge is greatly increased. Recent studies highlight sludge carbonization (Yadav *et al.* 2025) for its operational benefits, including minimal land use, reduced infrastructure expenditure, and near-zero pollutant emissions(Huang *et al.* 2021).

Municipal sludge and corn cob, as typical urban, agricultural and forestry solid waste pollutants, are ideal raw materials for the preparation of carbon products. After drying, the moisture content and volume of corn cob sludge are significantly reduced, and biochar can be prepared after pyrolysis and carbonization. Carbonizations have large pore size and specific surface area, rich surface functional groups, and can be used as good adsorbent materials (Pellenz *et al.* 2023), and have great potential for utilization in liquids, gases and decolorization. As the basis for the theoretical research and engineering application of sludge-based biochar, the carbonization process (Sharma *et al.* 2020) technology is: Solve sludge with corn (Wang *et al.* 2019). A powerful plan for the core pollution problem, and the treatment route of "treating waste with waste" is expected to be realized.

Sludge carbonization technology can be divided into high-temperature carbonization (Wang *et al.* 2022), medium-temperature carbonization(Liu *et al.* 2024) and low-temperature carbonization (Hossain *et al.* 2011) according to the difference in the final temperature of treatment and whether it is pressurized. If the high-temperature carbonization technology is used reasonably to treat urban sludge, optimized product will be obtained. Because it can directly use the calorific value of the sludge and the compounds produced in the carbonization furnace to support the front-end drying operation during the operation, it can save energy and reduce the generation of greenhouse gases (Markandya *et al.* 2009) such as CO_2. More than 95% of the heavy metals (Mendez *et al.* 2009) in sludge organic waste (Faria *et al.* 2018) can be converted into crystalline state with carbon after high-temperature carbonization treatment and solidified in carbon products. And because this technology can dry the sludge and pyrolysis is complete, it can increase the level of sludge reduction and achieve the purpose of harmlessness(Wang *et al.* 2019) and resource utilization (Chen *et al.* 2012) after treatment. Therefore, high-temperature carbonization technology has high application value (Singh *et al.* 2020).

This project intends to determine the physical and chemical indexes of high-temperature carbonized solid products under optimal reaction conditions (Pavlík *et al.* 2016), and comprehensively and systematically understand their basic properties, which is of great research significance for grasping the variation direction of high-temperature carbonized solid products and optimizing their resource performance. At the same time, in order to further illustrate the practical application value of the high-temperature carbonization prepared in this experiment, the optimal product was used to adsorb COD, ammonia nitrogen and total phosphorus in sewage (Ding *et al.* 2012), and compared with similar products, the water quality indexes (Zahedi 2017) before and after treatment were determined, and the adsorption mechanism of high-temperature carbonization will be discussed (Liu *et al.* 2009).

2. Materals and Methods

2.1. Materials

The raw materials used in this high-temperature carbonization (Xu *et al.* 2017) experiment consist of a mixture of sludge and corn cob. The sludge comes from a sewage treatment plant in Jingkou District, Zhenjiang City, Jiangsu Province , and it has undergone a drying operation. The corn cob was sourced from a local farm, and after being crushed and shifted, the powder had a particle size of 1 mm, and the powder was directly applied to this study.

2.2. Methods

A mixture of 35 g of sludge and corn cob (W_{sludge}:$W_{corn\ cob}$ = 4:1) was weighed and transferred to a porcelain boat. The experiment was carried out with a tube electric furnace, model SK-G08123K-610. The porcelain boat was placed in a tube furnace, and the pyrolysis (Wang *et al.* 2016) temperature (800 °C), heating rate (5 °C/min) and holding time (120 min) were set, respectively. The mixture is pyrolyzed at high temperature in a nitrogen atmosphere (Racek *et al.* 2020). The final cooled product is the corn cob-sludge high-temperature carbonization. In addition, pure sludge high-temperature carbonization was prepared under the same conditions described above for comparison.

2.3. Characterization

The surface morphology and structure of high-temperature carbonization samples were characterized and analyzed by an electron scanning microscope model Sigma 300 produced by ZEISS in Germany. The nitrogen adsorption and desorption behavior of high-temperature carbonization samples was tested using a BET specific surface area analyzer model Tristar 3020 manufactured by Micromeritics Instrument Corporation in the United States. An X-ray diffractometer model X'-PertPRO from PANalytical B.V., the Netherlands, was used to analyze the phase composition of the high-temperature carbonization samples.

2.4. Adsorption experiments

2.4.1. High-temperature carbonization adsorption COD experiment

In the dosage experiment, 0.4 g, 0.6 g, 0.8 g, 1.0 g, 1.2 g, and 1.4 g of material were added to 100 ml of COD

solution with a concentration of 300 mg/L, respectively. Place the mixed solution in a thermostatic shaking incubator with set temperature (25 °C), rotational speed (150 r/min), and shaking time (120 min). The solution after the reaction was taken out, the remaining COD concentration was measured, and the removal rate and adsorption capacity were calculated for details on how to determine COD concentration, see Supplementary Information (SI 1).

The adsorption time experiment was to add 1 g of material to 100 ml of COD solution at a concentration of 300 mg/L. The mixed solution was placed in a constant temperature shaking incubator with a set temperature of 25 °C and a rotation speed of 150 r/min, and samples were taken at the shaking times of 10 min, 20 min, 40 min, 60 min, 90 min, 120 min, 180 min and 240 min, respectively, and the mixed solution was taken out after the reaction to determine the remaining COD concentration. Calculate the removal rate as well as the adsorption capacity.

In different initial concentrations and temperature experiments, the prepared concentrations were 30 mg/L, 50 mg/L, 100 mg/L, 200 mg/L, 300 mg/L, 400 mg/L, and 600 mg/L, 800 mg/L COD solution, take 100 ml of solution respectively, add 1 g of material, and place the mixed solution in a constant temperature shaking incubator with set temperatures of 15 °C, 25 °C, 35 °C, rotation speed of 150 r/min, and shaking time of 120 min. The solution at the end of the reaction was removed, the remaining COD concentration was measured, and the removal rate and adsorption capacity were calculated.

2.4.2. Experiments on NH_4^+-N adsorption by high-temperature carbonization

The dosage experiment was performed by adding 0.4 g, 0.6 g, 0.8 g, 1.0 g, 1.2 g, and 1.4 g of the material to 100 ml of NH_4^+-N solution with a concentration of 40 mg/L, respectively. The mixed solution was placed in a thermostatic shaking incubator and the temperature (25℃), rotational speed (150 r/min) and shaking time (120 min) were set. The solution at the end of the reaction was removed and the remaining NH_4^+-N concentration was determined to calculate the removal rate as well as the adsorption capacity. The specific method for the determination of NH_4^+-N concentration is described in Supplementary Information (SI 2).

The adsorption time experiment was to add the material to 100 ml of NH_4^+-N solution with a concentration of 40 mg/L, place the mixed solution in a constant temperature shaking incubator, set the temperature at 25 °C, rotate at 150 r/min, and take samples at the shaking times of 10 min, 20 min, 40 min, 60 min, 90 min, 120 min, 180 min, and 240 min, respectively. After the reaction, the mixed solution was taken out, the remaining NH_4^+-N concentration was measured, and the removal rate and adsorption capacity were calculated.

In the experiments with different initial solution concentrations and temperatures, NH_4^+-N solutions with concentrations of 5 mg/L, 10 mg/L, 20 mg/L, 30 mg/L, 40 mg/L, 60 mg/L, 80 mg/L, and 100 mg/L were prepared, and 100 ml of solution was taken and 0.8 g of the material was added, respectively, and the mixed solution was placed in a constant temperature shaking incubator, and the temperatures were set at 15 ℃, 25 ℃, 35 ℃, rotational speed was 150 r/min, and shaking time was 120 min. The solution at the end of the reaction was taken out to determine the remaining NH_4^+-N concentration, and the removal rate as well as the adsorption capacity were calculated.

2.5. Data Analysis

2.5.1. Adsorption kinetics

To better understand solute adsorption behavior on high-temperature carbonizations, dynamic models are applied to quantify uptake rates and reveal adsorption mechanisms by fitting experimental data. Under isothermal conditions, the adsorption rate of porous materials is controlled by the speed of three basic processes:1.the velocity of the adsorbate molecules in the liquid film on the surface of the adsorbent particles;2.diffusion velocity within the adsorbent particles;3. the adsorption velocity of the pore surface within the adsorbent particle. Models commonly used to describe the adsorption process include Pseudo-first order kinetic models, Pseudo-second order kinetic models, and intragranular diffusion models. The relevant equations and parameters involved in adsorption kinetics are detailed in Supplementary Information (SI 3).

3. Results and Discussion

3.1. Material Analysis

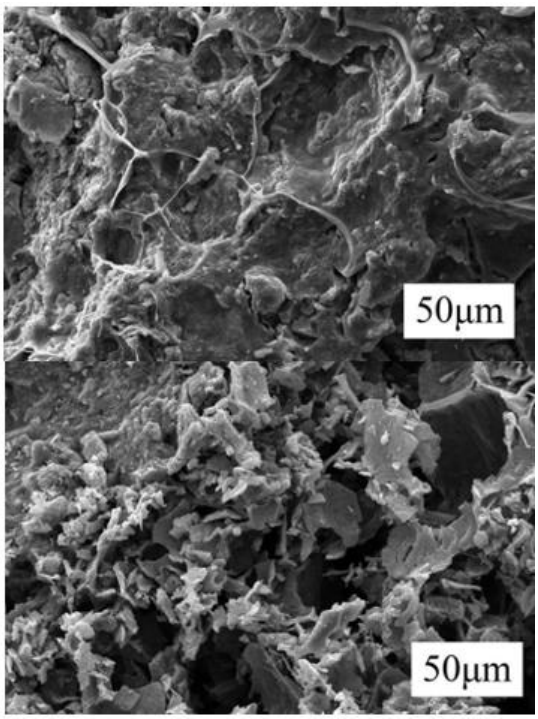

Figure 1. Scanning electron microscopy (SEM) images of high-temperature carbonized sludge and high-temperature carbonized corn cob-sludge mixture

As can be seen from **Figure (1)**, compared with the high-temperature carbonization of pure sludge, the corn cob-

sludge high-temperature carbonization exhibits a honeycomb structure with more developed overall pores, indicating that the addition of corn cob has a significant impact on the microscopic morphology of pure sludge high-temperature carbonization and is conducive to the development of its pore structure. In the process of high-temperature carbonization, with the volatilization and removal of different contents of cellulose, hemicellulose and other substances, the microscopic morphology of sludge-based high-temperature carbonization was changed, and a variety of different pore structures were formed, which increased the adsorption potential of high-temperature carbonization.

Table 1. Comparison of the pore structure of SSC and SJC

Category	SBET（m^2/g）	Vt（cm^3/g）	D(nm)
SSC	56.412	0.1383	10.081
SJC	166.399	0.3341	7.071

Notes:1. S_{BET}:BET specific surface area; V_t:total pore volume; D:Average pore size.

It can be seen from the table that the performance of SJC was significantly higher than that of SSC in terms of specific surface area, total pore volume and average pore size, and the addition of corn cob could significantly increase the specific surface area of high-temperature carbonization (increase by 194.97%), increase the total pore volume (increase by 141.57%) and decrease the average pore size (decrease by 29.86%).

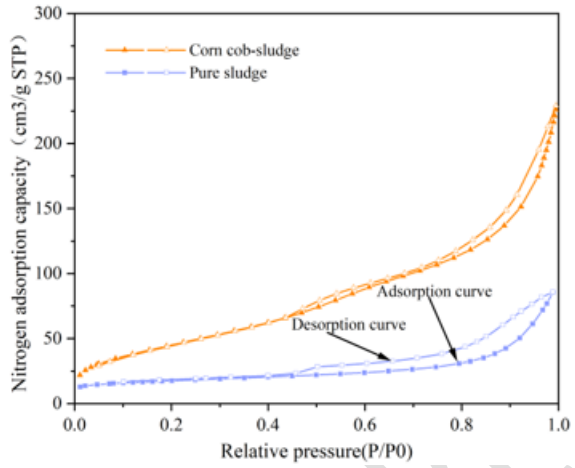

Figure 2. N_2 adsorption-desorption curves of high-temperature carbonized sludge and high-temperature carbonized corn cob-sludge mixture.

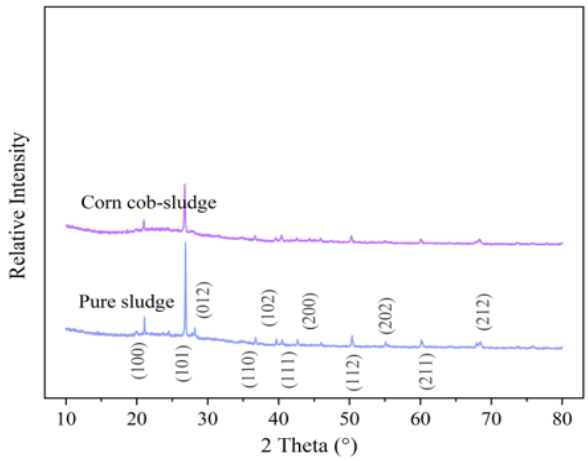

Figure 3. XRD spectra of high-temperature carbonization of corn-cob sludge

In **Figure 2**, The corn cob-sludge derived carbon exhibits a Type IV nitrogen adsorption isotherm, with low-pressure region hysteresis suggesting strong nitrogen affinity and a microporous structure. At the same time, there is an obvious separation phenomenon in the adsorption-desorption curve, indicating the existence of many micropores and mesopores. In addition, there is a large hysteresis ring in the figure, which is close to the H4 type, indicating that there are many slit-shaped pores or fractured pores composed of flake particles in the products generated by high-temperature carbonization.

As can be seen from **Figure 3**, the corn cob-sludge high-temperature carbonization has a broad peak at 2θ=22°, as well as a significant diffraction peak. The analysis of the XRD data by MDI jade shows that the crystals are mainly composed of SiO_2, and the obvious SiO_2 (101) diffraction peak can be seen around 2θ=26.6°. The signal intensity of this diffraction peak is higher than that of the standard SiO_2 diffraction peak, which is presumed to be due to the formation of graphite with a microcrystalline structure after high-temperature carbonization of the original organic matter in the sludge, and the microcrystalline structure is chaotic rather than ordered, which is consistent with the previous study (Xiao *et al.* 2014).In general, the SiO_2 diffraction peak of high-temperature carbonized sludge decreased significantly with the addition of corn cob, and the decrease intensified with the increase of the proportion of corn cob. When the corn cob is used as the conditioning agent, the 4:1 ratio of high-temperature carbonization has the lowest SiO_2 diffraction peak, which is due to the presence of SiO_2 crystals in pure corn cob, but the content is slightly lower, which means that the increase of the proportion of corn cob does not make the SiO_2 diffraction peak continue to decrease, but there is an extreme value.

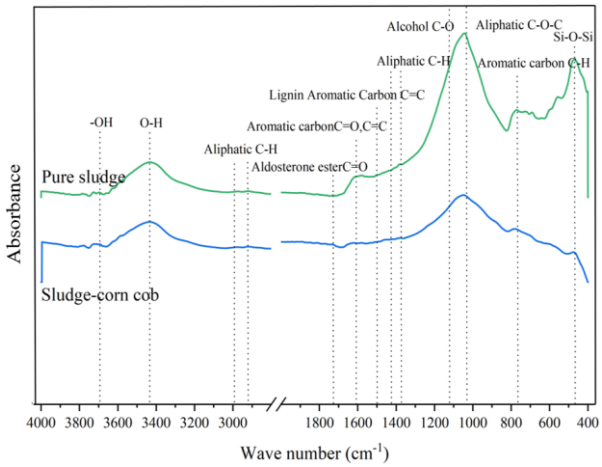

Figure 4. Infrared spectrogram of high-temperature carbonization of dried sludge and dried corn-cob sludge

In **Figure 4**, there are obvious absorption peaks of lignin and cellulose components at 700 cm^{-1} ~1600 cm^{-1}, and the vibrational absorption peaks between 1500 cm^{-1} ~1640 cm^{-1} are mainly from lignin structure, indicating that the lignocellulose-rich polymers in corn cobs are mainly from the lignin structure. 788 cm^{-1} ~881 cm^{-1} and 1612 cm^{-1} ~1615 cm^{-1} represent the C-H and C=C and C=O vibrations of aromatic carbonizations, respectively. The signal intensities at 2924 cm^{-1} ~2927 cm^{-1}, 2856 cm^{-1} ~2860 cm^{-1} and 1730 cm^{-1} ~1734 cm^{-1} represent the elastic vibrations of aliphatic C-H and hydroxyl, aldehyde, ketone and ester groups C=O in the polymer, respectively, indicating that the aliphatic and aldehyde ketone esters in the sludge have been fully degraded under the condition of high temperature carbonization. The structure of aliphatic functional groups will be removed with the dimethoxy and dehydration process of lignocellulose, while the C=O of hydroxyl, aldehyde, ketone and ester groups will be derived from sugars, and the sugars and cellulose will be basically degraded at more than 400 °C.

3.2. Study on the adsorption effect of COD by high-temperature carbonization

In order to make a significant comparison, corn cob-sludge high-temperature carbonization (SJC) and pure sludge high-temperature carbonization (SSC) under the same conditions were prepared and the adsorption performance was tested and analyzed under the same conditions. Based on the actual pollutant concentration range of domestic sewage, static adsorption simulates COD and NH_4^+-N in sewage (Wu *et al.* 2017).

3.2.1. Effect of dosage on COD adsorption effect

Different masses of SJC and SSC were added to the water at 25 °C, pH=7 and COD concentration of 300 mg/L, respectively. **Figure 5** shows the removal of COD by SJC and SSC under different dosages.

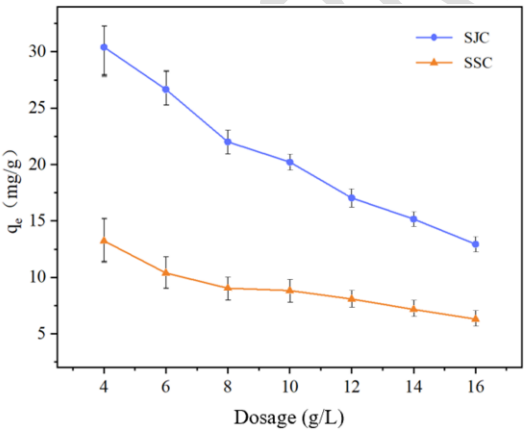

Figure 5. Effect of dosage on COD adsorption by high-temperature carbonization

Figure 5 demonstrates the superior COD removal efficiency of SJC compared to SSC. Both materials exhibited a decline in adsorption capacity with increasing dosage. At 4 g/L, SJC and SSC reached their maximum unit adsorption capacities (30.408 mg/g and 13.230 mg/g, respectively). However, at 16 g/L, these values decreased to 12.941 mg/g for SJC and 6.300 mg/g for SSC. This trend can be attributed to the inverse relationship between adsorbent concentration and unit adsorption area under constant COD conditions: as the total adsorption area expands with higher adsorbent dosage, the effective adsorption area per unit mass diminishes.

The removal of COD by both SJC and SSC showed an increasing trend when the dosage was increased from 4 g/L to 16 g/L. The removal of COD by SJC increased from 40.54% to 69.92%, and the removal of COD by SSC increased from 17.64% to 33.59%, which was probably due to the consequent increase of adsorption sites in the high-temperature carbons with the increase of the dosage. However, when the dosage was increased from 10 g/L to 16 g/L, the removal of COD by SJC increased by 0.76%, 1.63% and 0.14%, respectively, and that of COD by SSC increased by 2.89%, 1.09% and 0.18%, respectively, which were relatively small increases. The removal rates of SJC and SSC for COD basically reached equilibrium at the dosage of 10 g/L. The results showed that the removal rate of COD by SJC and SSC at high temperatures was higher than that of SSC. This indicates that the dosage of high-temperature carbons is not the more the better when removing COD. And with the increase of the dosage, it will lead to the increase of filtrate color. Therefore, the dosage of SJC and SSC was selected as 10 g/L in the subsequent experiments.

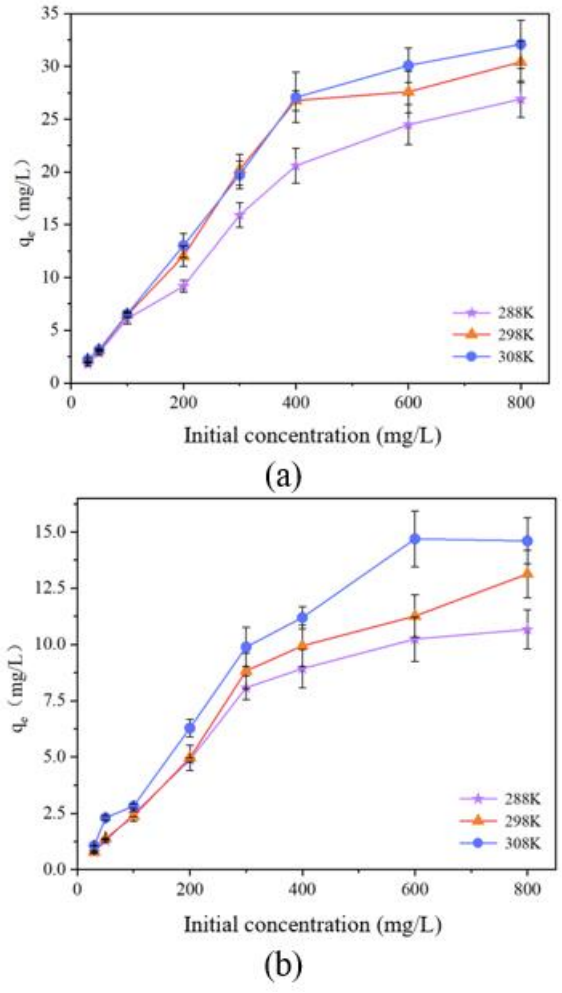

Figure 6. Effect of initial concentration and temperature on the adsorption of COD by high-temperature carbonizations: （a） Adsorption effect of SJC on COD;（b） Adsorption effect of SSC on COD

3.2.2. Effect of initial concentration and temperature on the adsorption effect of COD

The COD concentration range in the domestic sewage discharged into the urban sewage treatment plant is generally 200 mg/L ~400 mg/L, and the maximum is not more than 1000 mg/L, so the maximum simulated COD concentration in this paper is set at 800 mg/L. SJC and SSC were added to the COD water at pH=7 at different initial concentrations at a dosage of 10 g/L. **Figures .2(a)(b)** show the removal of COD at different initial concentrations by SJC and SSC at 288 K (15 °C), 298 K (25 °C), and 308 K (35 °C), respectively.

As can be seen from **Figure 6**, the adsorption capacity of SSC and SJC on COD increases with the increase of solution concentration, which indicates that the solution concentration has a great influence on the adsorption of high-temperature carbonization. When the initial concentration of COD is low, its adsorption capacity is also low, mainly due to the adsorbent not reaching saturated adsorption. This is because the higher the concentration of the solution, the greater the concentration difference between the solution itself and the high-temperature carbonization liquid film, which leads to an increase in the driving force of the migration of the adsorbate to the surface of the high-temperature carbonization, thereby increasing the adsorption capacity. Therefore, the appropriate increase of COD concentration is conducive to the adsorption of high-temperature carbonization. However, when the initial concentration of COD exceeds a certain limit, the adsorption capacity tends to be stable, which is due to the adsorption site on the high-temperature carbonization has been occupied and the adsorption reaches saturation.

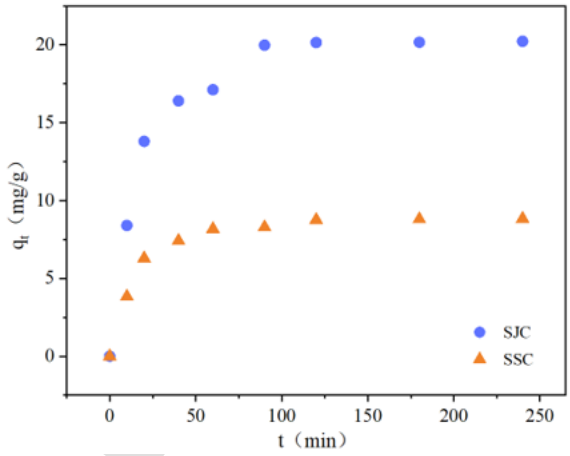

Figure 7. Effect of adsorption time on the adsorption of COD by high-temperature carbonization

The adsorption capacity of COD by SSC and SJC increased with the increase of temperature. At 35 °C, the maximum adsorption capacity of SSC and SJC was 14.688 mg/L and 40.125 mg/L, respectively, which were 1.43 and 1.19 times of the maximum adsorption capacity at 15 °C, respectively. The diffusion of COD in the pores of high-temperature carbonization is an endothermic process, and the increase of temperature enhances the mobility of COD and decreases the diffusion resistance, thereby promoting the adsorption of COD. The increase of temperature enhances the interaction between the adsorbate and the adsorbent, and forms a new adsorption site, which increases the adsorption capacity. COD underwent a surface chemical reaction with the high-temperature carbonization surface material.

3.2.3. Effect of adsorption time on COD adsorption effect

SJC and SSC were added to the COD water at pH=7, the reaction temperature was 298 K (25 °C), and the initial concentration was 300 mg/L. Figure 7 shows the changes in the amount of COD adsorption by SJC and SSC over time.

As can be seen from **Figure 7**, the adsorption capacity of SJC is much greater than that of SSC, and the adsorption process of SJC and SSC can be divided into fast phase and slow (flat) phase. With the extension of adsorption time, the adsorption capacity of NH_4^+-N by SJC and SSC first increased rapidly, then increased slowly, and finally tended to a certain value and reached equilibrium. When the adsorption time reached 120 min, the adsorption capacity of SJC and SSC increased to 20.14 mg/g and 8.76 mg/g, respectively. This may be due to the small molecular spacing and strong interaction in the early stage of adsorption, and the van der Waals force plays a major role, thus affecting the molecular diffusion rate. When the adsorption time is 240 min, the adsorption capacity of SJC and SSC for COD tends to be constant, and the adsorption point is close to saturation. The results show that for porous materials such as high-temperature carbonizations, the adsorption time has a great influence on the adsorption effect of COD, and it is necessary to leave enough contact time to fully react.

3.3. Research on the effect of NH_4^+-N adsorption by high-temperature carbonization

3.3.1. Effect of dosage on the adsorption effect of NH_4^+-N

Different qualities of SJC and SSC were added to the water at 25 °C, pH=7, and NH_4^+-N concentration of 40 mg/L, respectively. **Figure 8** shows the removal of NH_4^+-N by SJC and SSC under different dosages.

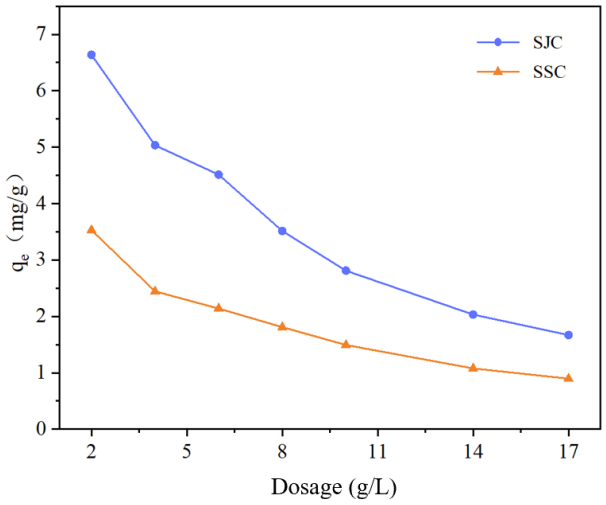

Figure 8. Effect of dosage on the adsorption of NH_4^+-N by high-temperature carbonization

As can be seen from **Figure 8**, the removal effect of SJC on NH_4^+-N is significantly better than that of SSC. The adsorption capacity of SJC and SSC for NH_4^+-N decreased with the increase of dosage, and when the dosage was 2 g/L, the adsorption capacity per unit of SJC and SSC was the largest, which was 6.636 mg/g and 3, respectively. 528 mg/g. When the dosage was increased to 17 g/L, the unit adsorption capacity of SJC and SSC decreased to 1.669 mg/g and 0.896 mg/g, respectively. This is due to the fact that when the volume of NH_4^+-N solution is constant with the initial concentration, with the increase of high-temperature carbonization concentration, the active point of binding to NH_4^+-N on the adsorbent surface increases, but the unsaturated surface also increases, and the adsorption capacity of NH_4^+-N per unit mass of high-temperature carbonization decreases.

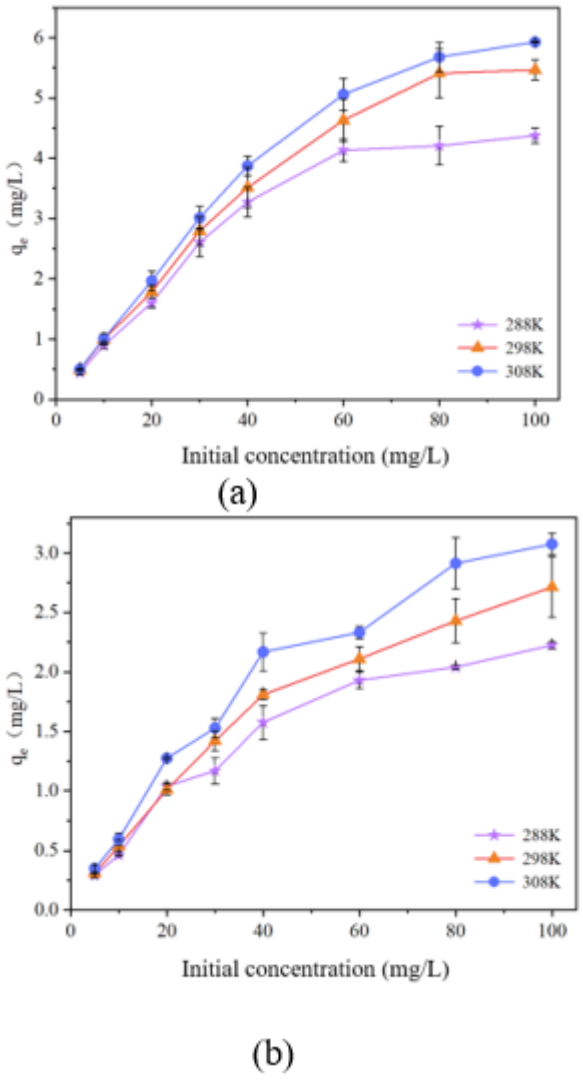

Figure 9. Effect of initial concentration and temperature on the adsorption of NH_4^+-N by high-temperature carbonization: (a) Adsorption effect of SJC on NH_4^+-N; (b)Adsorption effect of SSC on NH_4^+-N

When the dosage increased from 2 g/L to 17 g/L, the removal rate of NH_4^+-N by SJC and SSC showed an upward trend, the removal rate of SJC increased from 33.18% to 70.94%, and the removal rate of SSC increased from 17.64% to 38.09%, which was due to the increase of dosage The adsorption sites in the high-temperature carbonizations increase accordingly. When the dosage increased from 8 g/L to 17 g/L, the removal rate of NH_4^+-N by SJC increased by 0.029%, 0.846% and 0.228%, respectively. The removal rates of NH_4^+-N by SSC increased by 1.138%, 1.414% and 0.253%, respectively, and the increase was relatively small. At a dosage of 8 g/L, the removal rates of NH_4^+-N between SJC and SSC were basically balanced. The results indicated that the amount of high-temperature carbonization was not as much as possible when NH_4^+-N was removed. And with the increase of dosage, it will lead to an increase in the color of the filtration. Therefore, based on the above analysis, the dosage of SJC and SSC in the follow-up experiment was 8 g/L.

3.3.2. Effect of initial concentration and temperature on the adsorption effect of NH_4^+-N

The concentration range of NH_4^+-N in domestic sewage discharged into urban sewage treatment plants is generally 20 mg/L ~40 mg/L, and the maximum is not more than 100 mg/L, so the maximum simulated NH_4^+-N concentration in this project is set at 100 mg/L. SJC and SSC were added to NH_4^+-N water at pH=7 with different initial concentrations according to the dosage of g/L. **Figure 9(a)(b)** show the response of SJC and SSC to different initial concentrations of NH_4^+-N removal case at 288 K (15 °C), 298 K (25 °C), and 308 K (35 °C), respectively.

Figure 9 demonstrates that the NH_4^+-N adsorption capacity of SSC and SJC increases with higher solution concentrations. This trend is driven by the concentration gradient between NH_4^+-N in the solution and the carbon surface, which enhances the mass transfer driving force from the liquid to the solid phase. However, as the concentration exceeds a threshold, the active sites on both adsorbents become saturated, leading to adsorption equilibrium. These results highlight the significant influence of solution concentration on the adsorption performance of thermally modified carbons.

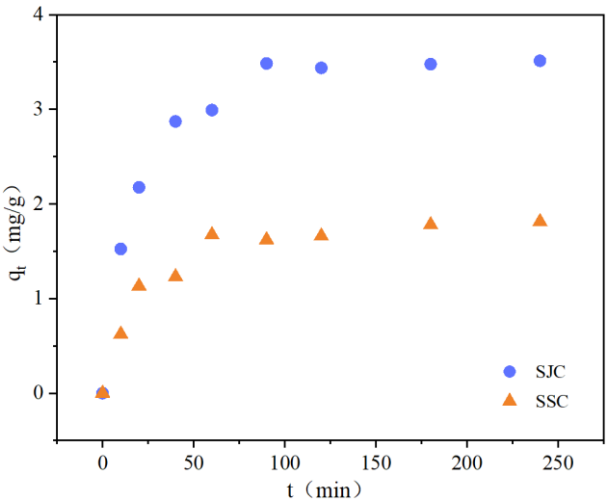

Figure 10. Effect of adsorption time on the adsorption of NH_4^+-N by high-temperature carbonization

The adsorption capacity of NH_4^+-N by SSC and SJC increased with the increase of temperature. At 35 °C, the maximum adsorption capacity of SJC and SSC was 5.93

mg/L and 3.08 mg/L, respectively, which were 1.35 and 1.28 times of the maximum adsorption capacity at 15 °C, respectively. Based on the previous speculation on the adsorption phenomenon of COD, increasing temperature also has a certain promotion effect on the adsorption of NH_4^+-N.

3.3.3. Effect of adsorption time on the adsorption effect of NH_4^+-N

SJC and SSC were added to NH_4^+-N water at pH=7, reaction temperature 298 K (25 °C), and initial concentration of 40 mg/L at a dosage of 10 g/L. The changes in the adsorption capacity of NH_4^+-N by SJC and SSC over time are shown in **Figure 10**.

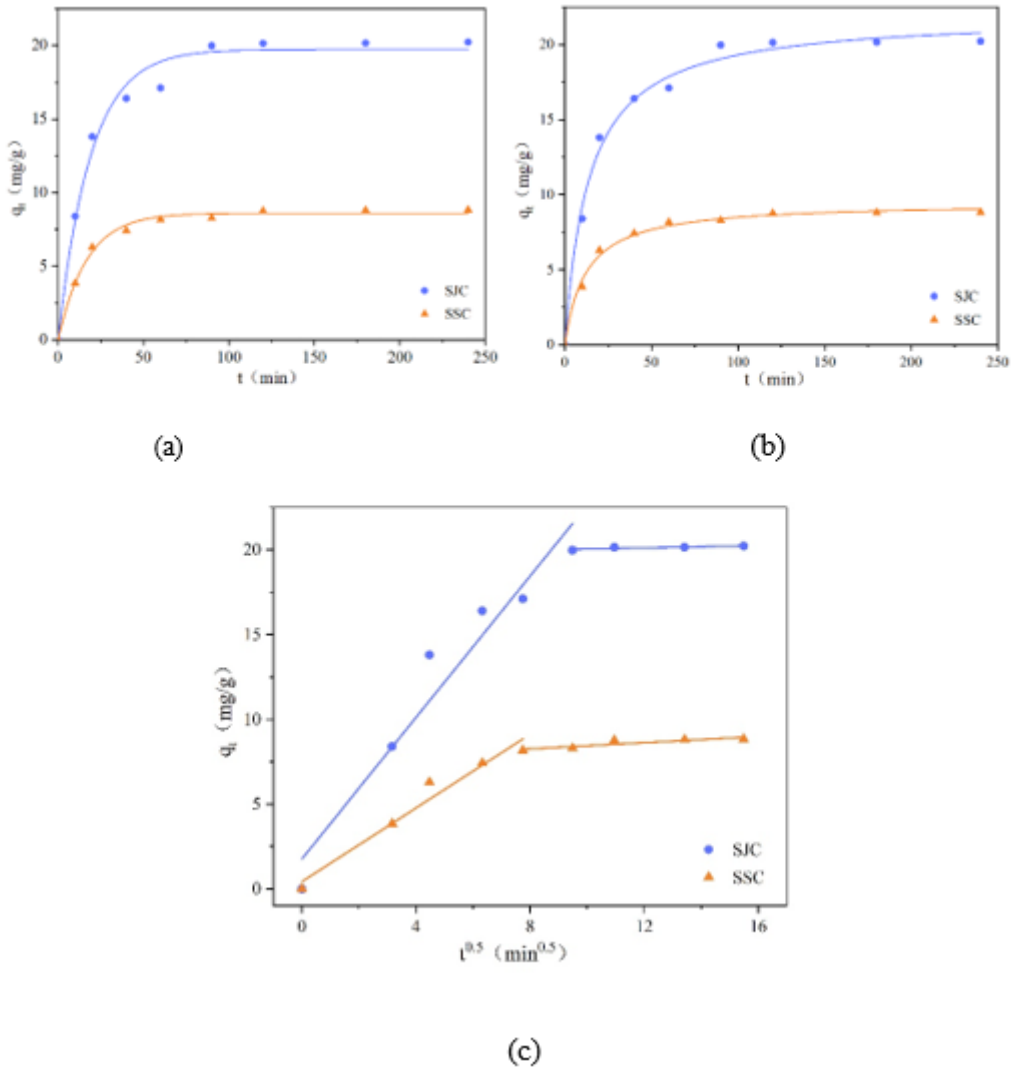

Figure 11. Fitting diagram of the kinetic model of COD adsorption by SJC and SSC: (a) Pseudo-first order kinetic model; (b) Pseudo-second order kinetic model （c） Intragranular diffusion model

As can be seen from **Figure 10**, the adsorption capacity of SJC is much larger than that of SSC, and the adsorption process of SJC and SSC can be divided into fast phase and slow (flat) phase. With the extension of adsorption time, the adsorption capacity of NH_4^+-N by SJC and SSC first increased rapidly, then increased slowly, and finally tended to be fixed and reached equilibrium. When the adsorption time reached 90 min, the adsorption capacity of SJC and SSC increased to 3.484 mg/g and 1.621 mg/g, respectively. This may be due to the small molecular spacing and strong interaction in the early stage of adsorption, and the van der Waals force plays a major role, thus affecting the molecular diffusion rate. When the adsorption time was 180 min, the adsorption capacity of NH_4^+-N by SJC and SSC tended to be fixed, which was speculated to be since the adsorption point was close to saturation. Similar to the adsorption of COD in the previous article, for porous materials such as high-temperature carbonizations, the adsorption time has a great influence on the adsorption effect of NH_4^+-N, and it is necessary to leave enough contact time to fully react.

3.4. Adsorption model fitting analysis

3.4.1. Adsorption kinetics

The adsorption dynamic model is used to describe the rate of adsorption of solutes by high-temperature carbonizations, and to explore the adsorption mechanism through the fitting analysis of the data. Under isothermal conditions, the adsorption rate of porous materials is controlled by the speed of three basic processes:①the

movement speed of the adsorbate molecules in the liquid film on the surface of the adsorbent particles; ②diffusion velocity within the adsorbent particles; ③adsorption velocity of the pore surface in the adsorbent particles. Models commonly used to describe the adsorption process include quasi-first-order kinetic models, quasi-second-order kinetic models, and intragranular diffusion models.

Table 2. Parameters of the fitting equation for the kinetic model of high-temperature carbonization adsorption of COD

category	Pseudo-first order kinetic model			Pseudo-second order kinetic model			Intragranular diffusion model		
	k_1	q_e (mg/g)	R^2	k_2	q_e (mg/g)	R^2	k_{id}	C'	R^2
SJC	0.0121	11.0790	0.9077	0.0038	21.5053	0.9902	1.2211	5.4926	0.7785
SSC	0.0109	4.6665	0.9455	0.4941	9.2851	0.9823	0.5180	2.6218	0.7454

Note: R^2 is the correlation coefficient

The adsorption data of SJC and SSC on COD were simulated by using Pseudo-first order kinetics, Pseudo-second order kinetics and intragranular diffusion models, and the fitting curves are shown in **Figure 11**.

The parameters of the linear fitting equation of the kinetic models of SJC and SSC adsorption COD are shown in **Table 2**.

Analysis of the kinetic model correlation coefficients (R^2) in **Table 2** reveals that the pseudo-second-order model provides the best fit for COD adsorption by both SJC and SSC. The calculated equilibrium adsorption capacities (q_e =21.5053 mg/g for SJC and 9.9823 mg/g for SSC) closely align with experimental values, further validating this model. These results suggest that the adsorption process is predominantly governed by chemisorption mechanisms.

At the same time, through **Figure 11(c)** The intragranular diffusion model can be seen at 0 min There are two straight sections in the time period of 0 min ~120min and 120min ~240min. The first straight segment has a high slope, indicating that the main adsorption during this period is external surface adsorption or transient adsorption, which also indicates that the mass transfer process in the early stage of adsorption is more realized by microporous diffusion, at the initial high concentration, the diffusion drive is strong and the adsorption rate is fast. The second segment of the straight line is relatively gentle, indicating that diffusion in the micropores has occurred, as the concentration decreases, the diffusion resistance dominates and the rate decreases, and adsorption may lead to particle swelling, pore collapse, or changes in surface functional groups (e.g., pH-responsive materials), which can change the subsequent diffusion path, and this process is also the velocity-controlled step of the whole adsorption process. Combine **Table 2** shows that $C' \neq 0$, that is, the fitting curve is not the origin, which indicates that SJC and SSC are not the only rate control step in the process of intragranular diffusion in the adsorption process of COD, and the whole adsorption process is the result of a variety of kinetic mechanisms, such as surface adsorption, ion exchange adsorption, liquid film diffusion, etc.

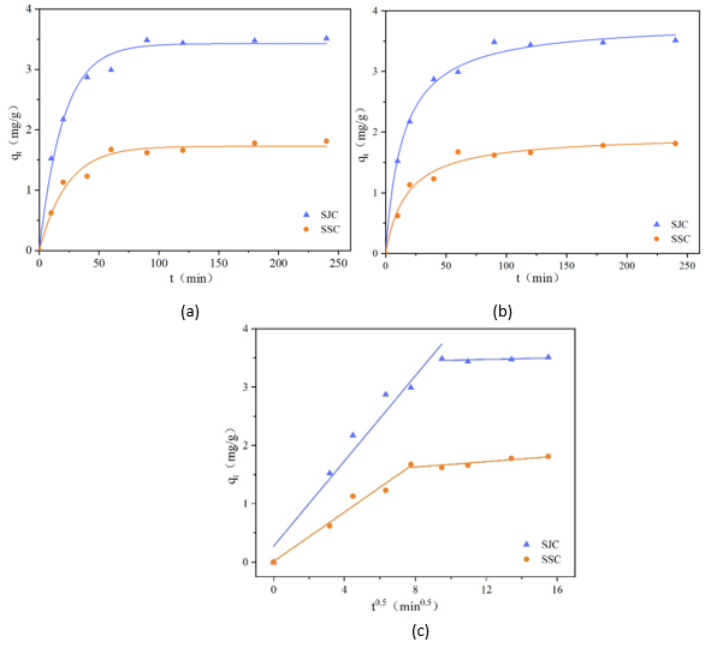

Figure 12. Fitting diagram of the kinetic model of adsorption of NH_4^+-N by SJC and SSC; (a) Pseudo-first order kinetic model; (b) Pseudo-second order kinetic model; (c) Intragranular diffusion model

The adsorption data of NH_4^+-N by SJC and SSC were simulated using Pseudo-first order kinetics, Pseudo-second order kinetics and intragranular diffusion models, and the fitting curves are shown in **Figure 12**.

The parameters associated with the linear fitting equations of the kinetic model for NH_4^+-N adsorption by SJC and SSC are shown in **Table 3**.

Figure 12 indicates that the pseudo-second-order kinetic model provides a superior fit for NH_4^+-N adsorption data of SJC and SSC compared to the pseudo-first-order model. As summarized in **Table 3**, the correlation coefficients (R^2) for the pseudo-second-order kinetics exceed 0.98., and the calculated values of saturated adsorption (q_e =3.7285 mg/g and 1.9489 mg/g) were more consistent with the actual experimental data. These results indicate that the adsorption of NH_4^+-N on high-temperature carbonizations SJC and SSC is more in line with the Pseudo-second order kinetic model, and the rate-controlled step of the adsorption process may be chemisorption.

As can be seen from the intragranular diffusion model in **Figure 12(c)**, there are two straight lines in the time period of 0min ~90min and 90min ~240min, respectively. Similar to the COD adsorption process, the first straight line has a high slope and the second straight line has a gentle slope, indicating that diffusion in the micropores has occurred, and this process is also the velocity-controlled step of the whole adsorption process. Combined with the fitting parameters in **Table 3**, it can be seen that $C' \neq 0$ the fitting curve is not the origin, indicating that the intra-particle diffusion of SJC and SSC is not the only rate control step in the adsorption process of NH_4^+-N, and the whole adsorption process is the result of a variety of kinetic mechanisms, such as surface adsorption, ion exchange adsorption, liquid film diffusion, etc.

Table 3. Parameters of the fitted equations for the kinetic model of NH_4^+-N adsorption by high temperature carbonization

category	Pseudo-first order kinetic model			Pseudo-second order kinetic model			Intragranular diffusion model		
	k_1	q_e (mg/g)	R^2	k_2	q_e (mg/g)	R^2	k_{id}	C'	R^2
SJC	0.0104	1.8802	0.8805	0.0215	3.7285	0.9917	0.2127	0.9287	0.7892
SSC	0.0088	1.2432	0.9453	0.0287	1.9489	0.9803	0.1118	0.3990	0.8170

Note: R^2 is the correlation coefficient

4. Conclusion

SEM shows that the addition of corn cob significantly affected the microscopic morphology of pure sludge high-temperature carbonization and contributed to the development of pore structure. BET pore structure analysis shows that the addition of corn cob could significantly increase the specific surface area of high-temperature carbonization (increase by 194. 97%), increase the total pore volume (increase by 141.57%) and decrease the average pore size (decrease by 29.86%). XRD shows that the SiO_2 diffraction peak of high-temperature carbonized sludge decreased significantly with the addition of corn cob, and the decrease intensified with the increase of the proportion of corn cob.

The experimental results show that corn cob-sludge high-temperature carbonization (SJC) and pure sludge high-temperature carbonization (SSC).The optimal dosage for COD and NH_4^+-N adsorption was 10 g/L and 8 g/L, respectively. The adsorption amount was positively correlated with the dosage amount and reaction temperature and negatively correlated with the initial concentration of the solution. At 298 K, the removal rate of SJC for the initial concentration of 300 mg/L COD solution and 40 mg/L NH_4^+-N solution was more than 50%, and the removal rate of 40 mg/L NH_4^+-N solution was 70%. The adsorption equilibrium time of SJC and SSC for COD was about 120 min, and the adsorption equilibrium time for NH_4^+-N was about 90 min.

Compared with the high-temperature carbonization of rice husk and sludge, the specific surface area of high-temperature carbonization bet of rice husk and sludge is 159.94 m^2/g, while the specific surface area of SJC is 166.4 m^2/g (increase by 4.04%), and the specific surface area of sludge mixed with other conditioners is generally not higher than 150 m^2/g, and the high specific surface area of SJC indicates that it has better adsorption performance. Although it is much smaller than the specific surface area of commercial carbon (936 m^2/g), it can achieve 70% of the COD adsorption effect of commercial activated carbon under the same parameters, and the adsorption equilibrium time of SJC (≤120 min) is significantly lower than that of commercial activated carbon (>24 h), because the rich mesoporous structure gives them lower mass transfer resistance. Therefore, the application of SJC adsorption treatment for wastewater needs to combine the properties of the wastewater and fully utilize the selective and rapid adsorption characteristics of SJC for some large molecule pollutants, in order to replace traditional commercial activated carbon and achieve high-value applications of SJC.

The adsorption kinetic fitting results showed that the adsorption of COD and NH_4^+-N on SJC and SSC was a fast adsorption process, and the diffusion within the micropores was an important rate-controlling step of the whole adsorption process, and the whole adsorption process was subject to the joint action of multiple kinetic mechanisms (surface adsorption, ion exchange

adsorption, and intra-particle diffusion, etc.). Among them, the quasi-secondary kinetic model can more accurately describe the adsorption process of COD and NH_4^+-N by SJC and SSC, and the R^2 can reach more than 0.98.

5. Future direction and limitations

In this study, sludge and corn cob are combined with high-temperature carbonization treatment, and the product is reused in the field of sewage treatment, which fills the research gap, and the overall research idea implements the treatment route of "treating waste with waste", which expands a new direction for the resource utilization of sludge and corn cob. This study focused on the optimization of high-temperature carbonization operating conditions, the evaluation of the basic characteristics of high-temperature carbonizations, and the adsorption effect of NH_4^+-N and COD in simulated wastewater, but the discussion of the effects of high-temperature carbonization on other pollutants in sewage and actual sewage treatment was lacking. The application of high-temperature carbonizations in other environmental fields still needs to be studied. For example, the removal effect of gaseous pollutants dioxins and organic dyes in printing and dyeing wastewater. Currently prepared high-temperature carbons contain a certain amount of SiO_2, which may cause pore blockage, leading to a decrease in specific surface area and adsorption potential, and subsequent treatment of high-temperature carbons can be carried out by means of physical or chemical activation in order to improve their adsorption capacity. This study did not conduct in-depth analysis on the impact of other pollutants in wastewater on adsorption, and there was no relevant research on the regeneration of SJC.

Supplementary Information (SI 1).

Methods for the determination of COD

According to the environmental protection industry standard of the People's Republic of China (HJ/T 399-2007), the chemical oxygen demand (COD) content in simulated wastewater was determined by rapid digestion spectrophotometry.

Prepare potassium hydrogen phthalate COD standard series solution for use, that is, 0.665 ml of potassium dichromate solution (0.5 mol/L), 0, in a digestion tube 0.335 ml of mercury sulfate solution (0.24 g/ml), 4 ml of silver sulfate-sulfuric acid solution (10 g/L). Shake the prefilled mixed reagent well, open the lid of the digestion tube, and measure a certain volume of COD standard series solution along the inner wall of the tube and add it to the tube; Tighten the cap of the digestion tube and shake the solution in the tube, put it into the rapid digestion instrument, and heat it at 165 °C for 15 min. After cooling, the absorbance value was measured with a photometer at a wavelength of 440 nm and 600nm using water as the reference liquid, and the calibration curve was plotted. The absorbance of the water sample after subsequent high-temperature carbonization treatment was determined according to the above steps, and the measured COD value was calculated from the corresponding calibration curve.

Supplementary Information (SI 2).

Methods for the determination of NH_4^+-N

According to the environmental protection industry standard of the People's Republic of China (HJ/T 535-2009), the ammonia nitrogen content in simulated wastewater was determined by Nessler's reagent spectrophotometry.

Add 0.0 ml, 0.5 ml, 1.0 ml, 2.0 ml, 4.0 ml, 6.0 ml, 8.0 ml, and 10.0 ml of ammonia nitrogen standard working solution (10 μg/ml) to 8 50 ml colorimetric tubes, respectively, and add water to the reticle; Add 1 ml of potassium sodium tartrate solution (500 g/L) and shake well, then add 1 ml of Nessler's reagent and shake well; Among them, the preparation method of potassium sodium tartrate solution is as follows: 50 g of potassium sodium tartrate is added to 100 ml of water, heated and boiled, fully cooled to room temperature, and then diluted to 100 ml; Nessler's reagent was cooled to room temperature by adding 16 g of sodium hydroxide (NaOH) to 50 ml of water, weighing 7 g of potassium iodide and 10 g of mercuric iodide and dissolving them in water, stirring while adding to the above NaOH solution, and then adding water to dilute to 100 ml. Leave for 10min. At a wavelength of 420 nm, the absorbance was determined with water as a reference and a calibration curve was plotted. The absorbance of the water sample after subsequent high-temperature carbonization treatment was determined according to the above steps, and the measured ammonia nitrogen value was found by the corresponding calibration curve.

Supplementary Information (SI 3).

(1) *Pseudo-first order kinetic model*

The Pseudo-first order kinetic model assumes that the adsorbate concentration is proportional to the adsorption velocity, and the limiting factor of the adsorption velocity is the presence of intraparticle mass transfer resistance. The Pseudo-first order kinetic equation is suitable for describing the adsorption process of the ideal surface monolayer, and Equation 1 is the Pseudo-first order kinetic equation

$$\lg\left(q_e - q_t\right) = \lg q_e - k_1 t \quad (1)$$

Where q_e is the saturated adsorption amount of the adsorbate on the adsorbent, mg/g; q_t is the adsorption amount of the adsorbate at t time on the adsorbent, mg/g; k_1 is the rate constant of the first-order kinetic model, min^{-1}; t is the reaction time, min.

(2) *Pseudo-second order kinetic model*

The Pseudo-second order kinetic model assumes that the binary of the adsorbate concentration is proportional to the adsorption velocity, and the limiting factor of the adsorption rate is the adsorption mechanism. This model

describes all the processes in which the adsorption process encompasses adsorption, such as surface adsorption, ion exchange and other processes. Equation 2 Pseudo-second order kinetic equations (Pseudo-second order kinetic equation） :

$$\frac{t}{q_t} = \frac{1}{k_2 q_e^2} + \frac{t}{q_e} \quad (2)$$

Where q_e is the saturated adsorption amount of the adsorbate on the adsorbent, mg/g; q_t is the adsorption amount of the adsorbate at t time on the adsorbent, mg/g; k_2 is the rate constant of the first-order kinetic model, min^{-1}; t is the reaction time, min.

(3) *Particle diffusion model*

The Particle diffusion model, also known as the Weber-Morris model, describes the overall intra-particle diffusion effect, the limiting factor of the adsorption rate is the intra-particle diffusion, when the equation fits the straight line but the origin, it shows that the intra-particle diffusion is not the only rate control step, and the whole adsorption process is the result of the joint action of a variety of kinetic mechanisms. Equation 5.3 is the mathematical expression of the intragranular diffusion model.

$$q_t = k_{id} t^{0.5} + C' \quad (3)$$

where q_t is the adsorbed amount of adsorbate on the adsorbent at moment t, mg/g; k_{id} is the rate constant of the intraparticle diffusion model, mg/(g·$min^{0.5}$); t is the reaction time, min; and C' is the thickness of the boundary layer, mg/g.

References

Amen, R., Yaseen, M., Mukhtar, A., Klemeš, J. J., Saqib, S., Ullah, S., Al-Sehemi, A. G., Rafiq, S., Babar, M., Fatt, C. L., Ibrahim, M., Asif, S., Qureshi, K. S., Akbar, M. M., and Bokhari, A. (2020). Lead and cadmium removal from wastewater using eco-friendly biochar adsorbent derived from rice husk, wheat straw, and corncob. *Cleaner Engineering and Technology*, ***1***, 100006-.

Cai, M.Q., Hu, J.Q., Wells, G., Seo, Y., Spinney, R., Ho, S.H., Dionysiou, D. D., Su, J., Xiao, R., and Wei, Z. (2018). Understanding Mechanisms of Synergy between Acidification and Ultrasound Treatments for Activated Sludge Dewatering: From Bench to Pilot–Scale Investigation. *Environmental Science and Technology*, ***52(***7), 4313–4323.

Chen, H., Yan, S.-H., Ye, Z.-L., Meng, H.-J., and Zhu, Y.-G. (2012). Utilization of urban sewage sludge: Chinese perspectives. *Environmental Science and Pollution Research International*, ***19***(5), 1454–1463.

Chen, M., Li, X., Yang, Q., Zeng, G., Zhang, Y., Liao, D., Liu, J., Hu, J., and Guo, L. (2008). Total concentrations and speciation of heavy metals in municipal sludge from Changsha, Zhuzhou and Xiangtan in middle-south region of China. *Journal of Hazardous Materials*, ***160***(2), 324–329.

Ding, R., Zhang, P., Seredych, M., and Bandosz, T. J. (2012). Removal of antibiotics from water using sewage sludge- and waste oil sludge-derived adsorbents. *Water Research (Oxford)*, ***46***(13), 4081–4090.

Faria, W. M., Figueiredo, C. C. de, Coser, T. R., Vale, A. T., and Schneider, B. G. (2018). Is sewage sludge biochar capable of replacing inorganic fertilizers for corn production? Evidence from a two-year field experiment. *Archiv Für Acker- Und Pflanzenbau Und Bodenkunde*, ***64***(4), 505–519.

Hossain, M. K., Strezov, V., Chan, K. Y., Ziolkowski, A., and Nelson, P. F. (2011). Influence of pyrolysis temperature on production and nutrient properties of wastewater sludge biochar. *Journal of Environmental Management*, ***92***(1), 223–228.

Huang, X., Ding, A., Gao, J., Zheng, B., Zhou, D., Qi, X., Tang, R., Wang, J., Ren, C., Nie, W., Chi, X., Xu, Z., Chen, L., Li, Y., Che, F., Pang, N., Wang, H., Tong, D., Qin, W., … Qiang Zhang Kebin He. (2021). Enhanced secondary pollution offset reduction of primary emissions during COVID-19 lockdown in China. *National Science Review*.

Iheanacho, O. C., Nwabanne, J. T., Obi, C. C., Igwegbe, C. A., Onu, C. E., Dahlan, I., and Rather, S. (2023). Adsorptive Dephenolization of Aqueous Solutions Using Thermally Modified Corn Cob: Mechanisms, Point of Zero Charge, and Isosteric Heat Studies. *Adsorption Science and Technology*, *2023*.

Li, J., Lv, G., Bai, W., Liu, Q., Zhang, Y., and Song, J. (2016). Modification and use of biochar from wheat straw (Triticum aestivum L.) for nitrate and phosphate removal from water. *Desalination and Water Treatment*, ***57***(10), 4681–4693.

Liu, J., Jiang, X., Zhou, L., Han, X., and Cui, Z. (2009). Pyrolysis treatment of oil sludge and model-free kinetics analysis. *Journal of Hazardous Materials*, ***161***(2), 1208–1215.

Liu, S., Wei, G., Liu, H., Zhu, Y., Shi, H., & Lian, Y. (2024). From waste to resource: a multidimensional analysis of sewage sludge thermochemical treatment efficiency across temperatures. *Environmental Science Water Research & Technology*, ***1***(12), 3238–3248.

Mahapatra, K., Ramteke, D. S., and Paliwal, L. J. (2012). Production of activated carbon from sludge of food processing industry under controlled pyrolysis and its application for methylene blue removal. *Journal of Analytical and Applied Pyrolysis*, ***95***, 79–86.

Markandya, A., Armstrong, B. G., Hales, S., Chiabai, A., Criqui, P., Mima, S., Tonne, C., and Wilkinson, P. (2009). Health and Climate Change 3: Public health benefits of strategies to reduce greenhouse-gas emissions: low-carbon electricity generation. *The Lancet (British Edition)*, ***374***(9706), 2006-.

Mendez, A., Barriga, S., Fidalgo, J. M., and Gasco, G. (2009). Adsorbent materials from paper industry waste materials and their use in Cu(II) removal from water; Adsorbent materials from paper industry waste materials and their use in Cu(II) removal from water. *Journal of Hazardous Materials*, ***165***(1–3), 736–743.

Merzari, F., Langone, M., Andreottola, G., and Fiori, L. (2019). Methane production from process water of sewage sludge hydrothermal carbonization. A review. Valorising sludge through hydrothermal carbonization. *Critical Reviews in Environmental Science and Technology*, ***49***(11), 947–988.

Mozaffari Majd, M., Kordzadeh-Kermani, V., Ghalandari, V., Askari, A., and Sillanpää, M. (2022). Adsorption isotherm

models: A comprehensive and systematic review (2010−2020). *The Science of the Total Environment*, ***812***, 151334–151334.

Mubarak, N. M., Alicia, R. F., Abdullah, E. C., Sahu, J. N., Haslija, A. B. A., and Tan, J. (2013). Statistical optimization and kinetic studies on removal of Zn^{2+} using functionalized carbon nanotubes and magnetic biochar. *Journal of Environmental Chemical Engineering*, ***1***(3), 486–495.

Pavlík, Z., Fořt, J., Záleská, M., Pavlíková, M., Trník, A., Medved, I., Keppert, M., Koutsoukos, P. G., and Černý, R. (2016). Energy-efficient thermal treatment of sewage sludge for its application in blended cements. *Journal of Cleaner Production*, ***112***, 409–419.

Pellenz, L., de Oliveira, C. R. S., da Silva Júnior, A. H., da Silva, L. J. S., da Silva, L., Ulson de Souza, A. A., de Souza, S. M. de A. G. U., Borba, F. H., and da Silva, A. (2023). A comprehensive guide for characterization of adsorbent materials. *Separation and Purification Technology*, ***305***, 122435-.

Racek, J., Sevcik, J., Chorazy, T., Kucerik, J., and Hlavinek, P. (2020). Biochar – Recovery Material from Pyrolysis of Sewage Sludge: A Review. *Waste and Biomass Valorization*, ***11***(7), 3677–3709.

Selvanarayanan R., Rajendran S., Pappa C. K. and Thomas B. (2024), Wastewater recycling to enhance environmental quality using fuzzy embedded with rnn-iot for sustainable coffee farming, *Global NEST Journal*, **26**(8), 06346.

Suresh M., Surendran R., Raveena S., and Gowri S. (2025), Wastewater recycling integration with IoT sensor vision for real-time monitoring and transforming polluted ponds into clean ponds using HG-RNN, *Global NEST Journal*, 27(4), 06758.

Sánchez, M. E., Menéndez, J. A., Domínguez, A., Pis, J. J., Martínez, O., Calvo, L. F., and Bernad, P. L. (2009). Effect of pyrolysis temperature on the composition of the oils obtained from sewage sludge. *Biomass and Bioenergy*, ***33***(6), 933–940.

Sharma, H. B., Sarmah, A. K., and Dubey, B. (2020). Hydrothermal carbonization of renewable waste biomass for solid biofuel production: A discussion on process mechanism, the influence of process parameters, environmental performance and fuel properties of hydrochar. *Renewable and Sustainable Energy Reviews*, ***123***, 109761

Singh, S., Kumar, V., Dhanjal, D. S., Dhiman, J., Prasad, R., and Singh, J. (2020). A sustainable paradigm of sewage sludge biochar: Valorization, opportunities, challenges and future prospects. *Journal of Cleaner Production*, ***269***, 122 59-.

Venkatraman M., Surendran R., Srinivasulu S. and Vijayakumar K. (2024), Water quality prediction and classification using attention based deep differential recurflownet with logistic giant armadillo optimization, *Global NEST Journal*, 27(1), 06799

W.D., C. U., Veksha, A., Giannis, A., Liang, G., Hu, X., and Lim, T.-T. (2019). Insights into the speciation of heavy metals during pyrolysis of industrial sludge. *The Science of the Total Environment*, ***691***, 232–242.

Wang X. B., Deng S. H.,Tan H. Z.(2016). Synergetic effect of sewage sludge and biomass co-pyrolysis: A combined study in thermogravimetric analyzer and a fixed bed reactor. ENERGY CONVERSION AND MANAGEMENT, **118**, 399-405.

Wang Y, Li Z, Kong J.(2022). In situ wide-angle X-ray scattering study on the change of microcrystalline structure in Jincheng anthracite during high-temperature carbonization. *Journal of applied crystallography*, **55**(2), 265-270.

Yadav, V.,Shrotriya, S. (Eds.). (2025). Waste-To-Wealth : Resource Recovery and Value-Added Products for Sustainable Development ,First edition, CRC Press.

Zongshu. (2024). The fourth meeting of the Central Committee for Comprehensively Deepening Reforms emphasized promoting a comprehensive green transformation of economic and social development. *Jianzhu Jieneng = Construction Conserves Energy*, ***52***(2), 1.